CONTRASTING MINERAL ASSOCIATIONS BETWEEN TWO WOLLASTONITE-BEARING CALC-SILICATE GNEISSES, EASTERN SØR RONDANE MOUNTAINS, ANTARCTICA

Masao Asami[1], Edward S. Grew[2] and Hiroshi Makimoto[3]

[1]*Department of Geological Sciences, College of Liberal Arts, Okayama University, 1-1, Tsushima-naka 2-chome, Okayama 700*
[2]*Department of Geological Sciences, University of Maine, 5711 Boardman Hall, Orono, Maine 04469-5711, U.S.A.*
[3]*Geological Survey of Japan, 1-3, Higashi 1-chome, Tsukuba 305*

Abstract: Calc-silicate gneisses are found at Austhamaren and Eremitten in the polymetamorphic granulite- and amphibolite-facies metamorphic rocks of the eastern Sør Rondane Mountains. The diagnostic assemblage in the Austhamaren calc-silicate is garnet (Grt)-quartz (Qtz)-wollastonite (Wo)-calcite (Cal), whereas Wo-plagioclase (Pl)-scapolite (Scp)-Qtz and Wo-Cal-Scp-Qtz are characteristic assemblages in the Eremitten gneiss. Wollastonite and calcite are nearly end member $CaSiO_3$ and $CaCO_3$. The other major phases approach the calcic end members: garnet is 80-91 mole% grossular, plagioclase is An_{88-94}, and scapolite 77-83 mole% meionite. Clinopyroxene is hedenbergite ($Fe/(Fe+Mg)=0.50-0.67$). The reactions $Grt+Qtz=Wo+An$ and $Grt+CO_2=Wo+Scp+Cal$ relate the assemblages in the Austhamaren and Eremitten samples. The two assemblages could be interepreted to result from a regional pressure decrease from Austhamaren in the north to Eremitten in the south. An alternative interpretation is that the Eremitten Wo-Scp assemblages formed at somewhat higher CO_2 activities, and Wo-An, at a slightly higher bulk Na/Ca ratio, compared to the Austhamaren assemblage. X_{CO_2} ($=CO_2/(CO_2+H_2O)$ in the associated fluid phase) is estimated to have been buffered at <0.3 in the Eremitten rock and at 0.1-0.2 in the Austhamaren rock (for $T=760-800°C$, $P=7-8$ kbar). X_{CO_2} remained low during a near-isobaric temperature decrease to $T\leqslant 600°C$ following peak conditions at Eremitten when garnet selvages developed around wollastonite, scapolite, and plagioclase and scapolite was partially replaced by Pl+Cal+K-feldspar symplectite.

1. Introduction

Wollastonite is an important indicator mineral for metamorphic conditions. In contrast to the complex solid solutions of minerals which occur in the more abundant pelitic and mafic rocks, wollastonite and associated minerals in calc-silicate rocks are commonly close in composition to the calcic end members. Consequently, theoretical and experimental studies, notably the pressure-sensitive, vapor-absent reaction wollastonite + anorthite = grossular + quartz (*e.g.*, Windom and Boettcher, 1976), can be readily applied to wollastonite-bearing assemblages.

Wollastonite-bearing rocks are also sensitive indicators of fluid compositions ; *e.g.*, the assemblage wollastonite + garnet + scapolite in regionally metamorphosed rocks is an indication of relatively low CO_2 activities in the fluid phase (Harley and Buick, 1992).

In the eastern Sør Rondane Mountains, granulite-facies metamorphic rocks occur widely and locally include calcareous rocks (Asami *et al.*, 1989; Grew *et al.*, 1989a). Among these calcareous rocks, we found wollastonite-bearing calc-silicate gneisses at two different localities, one containing the grossular-rich garnet-quartz association and the other containing the wollastonite-anorthitic plagioclase associa- tion with retrograde reaction textures. The purpose of this paper is to describe petrographic characteristics and petrogenetic significance of the two gneisses.

2. Geologic Setting

The Sør Rondane Mountains (Fig. 1) are underlain by a migmatized gneissic complex, intruded by granitic and syenitic plutonic rocks. Most of the metamor- phic rocks were subjected to the medium-pressure type regional metamorphism which included a granulite-facies event with peak conditions of 750–800°C and 7–8 kbar and associated prograde and retrograde episodes (for the latter episode 530– 580°C and ～5.5 kbar has been estimated), and which was followed by a contact metamorphic event under low-pressure conditions (around 550°C and 3 kbar), mainly in the central part of the mountains (Asami *et al.*, 1992). The earlier, mostly granulite-facies, metamorphism has been dated by geochronological data at about 1000 Ma before present, and the later, low-*P* plutonic and metamorphic activity which followed uplift, at about 500 Ma before present (Asami *et al.*, 1992; Grew *et al.*, 1992; Shiraishi and Kagami, 1992). The *P-T-t* trajectory of the Sør Rondane metmorphism has been considered to be a clockwise path for the regional metamor- phism and a near-isothermal decompression path with subsequent isobaric heating during the contact metamorphism.

Geology of the eastern Sør Rondane Mountains and petrology and mineralogy of some metamorphic rocks in this area have been reported in detail by Grew *et al.* (1988, 1989a, b, 1991), Asami *et al.* (1989, 1990, 1991) and Makimoto *et al.* (1990). Basement rocks exposed in the map area are composed of high-grade gneissic rocks accompanied by migmatite and small bodies of intrusive rocks (Fig. 1). The majority of the metamorphic rocks are intermediate in composition, represented by biotite-hornblende gneiss, with subordinate pelitic, calcareous, quartzo-feldspathic, mafic and ultramafic rocks. Regional metamorphism in the granulite facies ～1000 Ma ago is indicated by the common occurrence of orthopyroxene- and two- pyroxene-bearing assemblages as shown in Fig. 1. The amphibolite-facies over- print, dated at ～500 Ma, is closely related to regional migmatization and has been recognized as a discrete event on the basis of geologic and petrologic features.

3. Field Occurrence

Wollastonite-bearing calc-silicate gneisses were found at Austhamaren (Sample
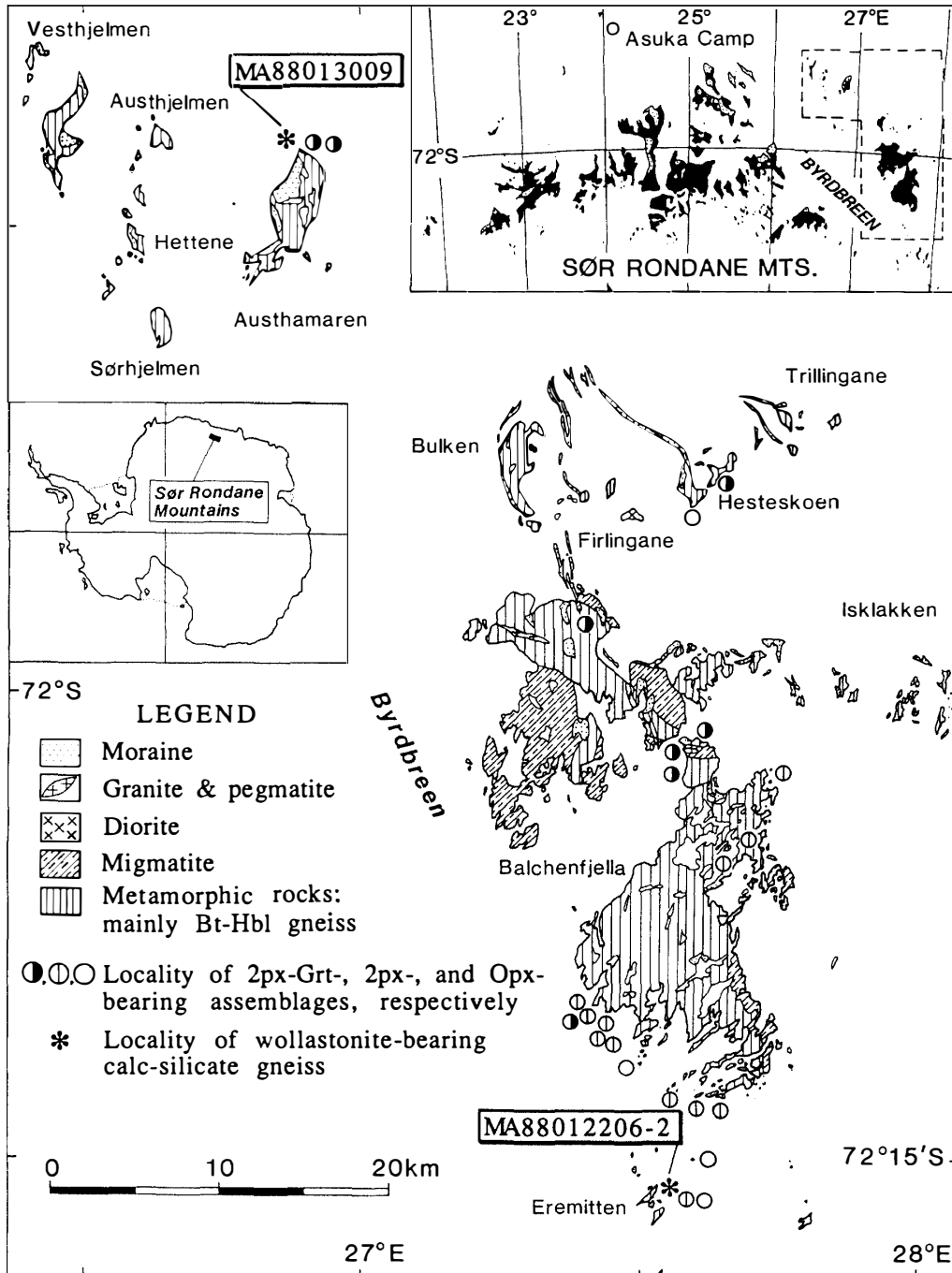
Fig. 1. Simplified geological map of the eastern Sør Rondane Mountains, showing lacalities of two wollastonite-bearing calc-silicate gneisses and orthopyroxene-bearing assemblages in intermediate and mafic metamorphic rocks. Modified from ASAMI et al. (1989, 1991).

1 : MA88013009), and at Eremitten (Sample 2 : MA88012206-2, Fig. 1).

The north end of Austhamaren is underlain by NNE-SSW-trending and easterly dipping, feldspathic to mafic garnetiferous gneisses and granulites, including garnet-hornblende gneisses and distinctive iron-rich fayalite-clinopyroxene-

ferrosilite-hornblende-almandine granulite, which are intruded by cummingtonite±
orthopyroxene orthogneiss and later by several metamorphosed garnetiferous dikes.
Marble containing blocks of silicate rocks forms a layer about 0.5 m thick under the
orthogneiss; a second marble 2 cm thick is found as a slice entirely enclosed in the
orthogneiss. The thicker marble is intercalated with the iron-rich granulite, but is
locally in direct contact with the orthogneiss. The marble appears to have flowed
and the blocks could be tectonic inclusions.

Wollastonite-bearing rocks are found not only with the thicker marble, but also
in a slice of finely layered calc-silicate rock in the orthogneiss between the two
marbles. Sample 1 was collected from an irregular lens up to about 20 cm thick
between the thicker marble and the overlying iron-rich mafic granulite (Fig. 2).
Layering in the calc-silicate lens appears to be locally truncated by the marble,
possibly as a result of flow. The lens is composed of light-gray wollastonite-bearing
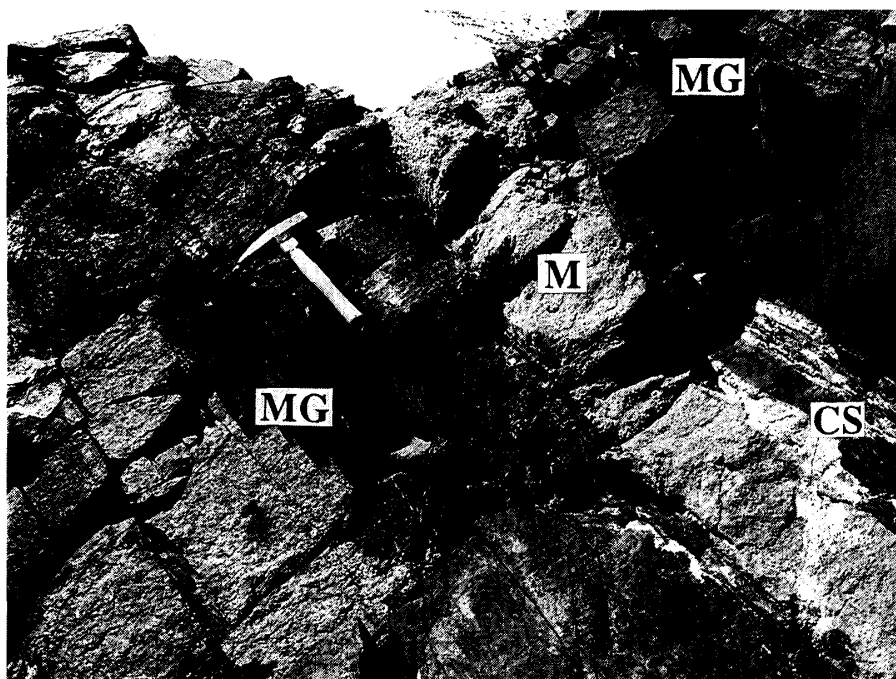
Fig. 2. Mode of occurrence of the wollastonite-bearing calc-silicate gneiss (Sample
1) in a marble layer at Austhamaren. The gneiss (CS) is in contact with
the marble (M) with an irregular boundary and is associated with thin
bands of garnet-clinopyroxene gneiss. The marble layer is intercalated in
iron-rich mafic granulite (MG).

Table 1.   Mineral assemblages of

	Sample No.	Locality	Domain	Wo	Grt	Cpx
1.	MA88013009	Austhamaren	A, B, C	+	+	+
2.	MA88012206-2	Eremitten	I	+	(+)	+
			II	+	(+)	+

— : Trace   in   amount.   ( ) : Secondary   product.   Mineral   abbreviations :
K-feldspar, Pl-plagioclase, Po-pyrrhotite, Py-pyrite, Qtz-quartz, Scp-scapolite,

gneiss, pale green or pale pink in places, and dark green bands of garnet-clinopyroxene gneiss developed parallel to the marble layer. The marble in contact with this lens contains minor quartz, clinopyroxene and scapolite, but no wollastonite. The slice of calc-silicate rock is associated with a metamorphosed dike cutting the orthogneiss a few centimeters above the thicker marble. In this slice, wollastonite-bearing layers alternate with layers containing the assemblages garnet-clinopyroxene,   scapolite-clinopyroxene-plagioclase,   and   hornblende-biotite-plagioclase-K-feldspar-clinopyroxene. Both calc-silicate rocks could have formed by reaction of marble with the orthogneiss.

At Eremitten, NE-SW-trending and southeasterly dipping, well-layered biotite-hornblende gneiss and subordinate amphibolite, both of which locally contain clinopyroxene-orthopyroxene assemblages, are found with charnockitic gneiss. Light brownish gray calc-silicate gneiss (Sample 2) forms a concordant layer 1–2 m thick in the biotite-hornblende gneiss.

Given the presence of metamorphic orthopyroxene at both localities, we infer that the calc-silicate gneisses were subjected to granulite-facies metamorphism. However, Sample 1 was probably also metamorphosed by the orthogneiss at the time it was emplaced, that is, the assemblage in Sample 1 could have resulted from the combined effects of an early contact event and of a subsequent regional, granulite-facies event.

4. Textural Relations and Mineral Assemblages

The wollastonite-bearing calc-silicate gneisses are fine- to medium-grained, and have compositional banding (gneissosity) represented by the difference in modal amount of minerals. Constituent minerals of these gneisses are listed in Table 1. The mineral abbreviations proposed by KRETZ (1983) are used in Table 1 and in describing mineral assemblages and reactions.

Sample 1 has an indistinctly foliated appearance due to the flattening of larger wollastonite and garnet grains, which are set in a matrix of finer-grained garnet, wollastonite, quartz, clinopyroxene, calcite, apatite, and titanite. The large garnet grains are poikilitic with inclusions of calcite, quartz, clinopyroxene, and wollastonite. Overall, the minerals appear to be in texural equilibrium, which suggests the stable assemblage Grt-Qtz-Wo-Cal-Cpx (Fig. 3a). Wollastonite is the phase most affected by alteration; it is embayed and cut by seams of fine-grained secondary minerals, possibly including calcite and quartz.

Sample 2 consists of two domains, which are distinguished by the presence or

wollastonite-bearing calc-silicate gneisses

Scp	Pl	Kfs	Qtz	Cal	Ttn	Ap	Py	Po	Ccp
		+	+	−	+	−	−		
+	+		+		+	−			−
+	(+)	(−)	+	+(−)	+	−			−

Ap-apatite, Cal-calcite, Ccp-chalcopyrite, Cpx-clinopyroxene, Grt-garnet, Kfs-Ttn-titanite, Wo-wollastonite.
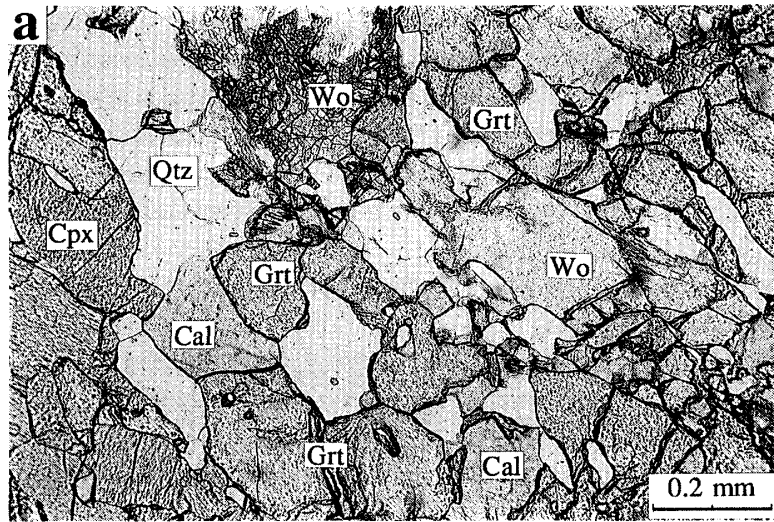
a. Sample 1 (MA88013009, Austhamaren). Garnet coexists with quartz, wollastonite, calcite and clinopyroxene. One nicol.
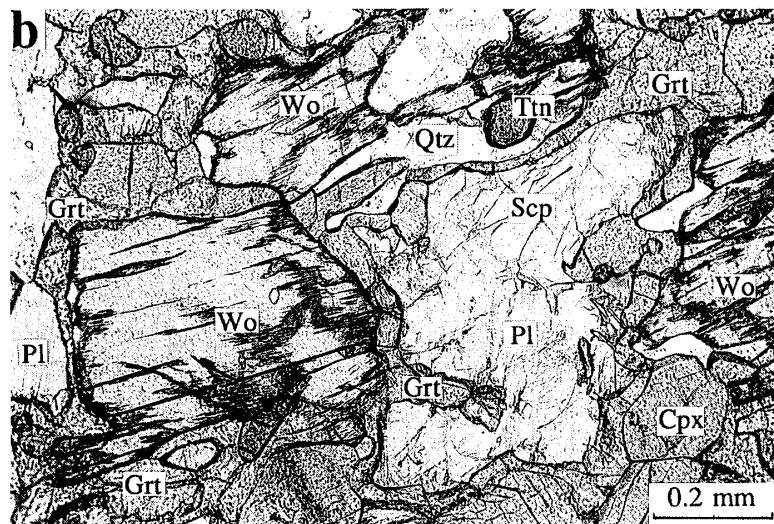
b. Domain I in Sample 2 (MA 88012206-2, Eremitten). Grains of wollastonite, plagioclase and scapolite are surrounded by garnet selvages. Other grains of wollastonite are intimately associated with quartz. Clinopyroxene and titanite are also seen as grains coexisting with wollastonite and quartz. One nicol.
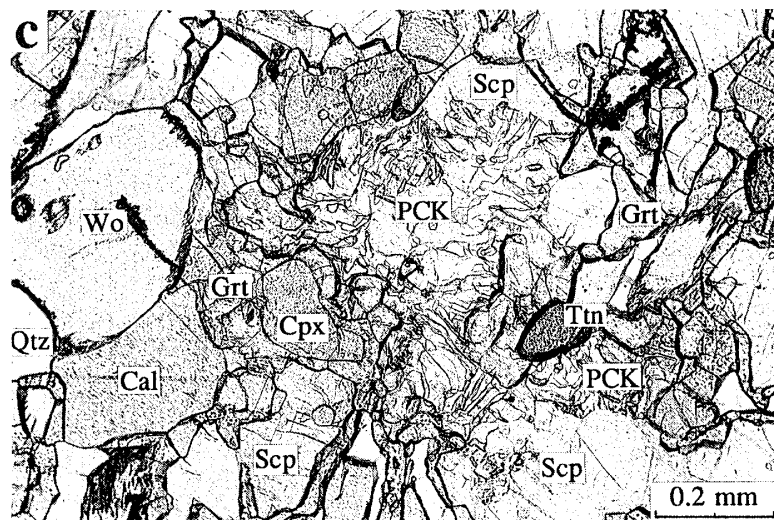
c. Domain II in Sample 2. Scapolite grains enclosed by garnet selvages are partially replaced by symplectic aggregates of plagioclase, calcite and K-feldspar (PCK). Wollastonite, calcite and quartz coexist with each other in this domain. One nicol.

Fig. 3. Photomicrographs of the wollastonite-bearing calc-silicate gneisses.

absence of calcite.   Wollastonite, quartz, plagioclase, scapolite, and clinopyroxene have a roughly equigranular texture in Domain I suggestive of equilibrium growth prior to development of garnet selvages (Fig. 3b).   The calcite-bearing assemblage Wo-Qtz-Cal-Scp-Cpx-Ttn-(Grt) (Domain II) was described in an another sample from this outcrop by GREW *et al*. (1989, MA88012206-1).   Sample 2 is characterized by the following textures:

(1)   Garnet selvages are developed along wollastonite-plagioclase, wollastonite-scapolite, and scapolite-calcite grain boundaries or around wollas-tonite, plagioclase, and scapolite (Fig. 3b).   In Domain I, wollastonite is never in contact with either plagioclase or scapolite, although plagioclase and scapolite locally are in contact, whereas in Domain II, scapolite is not in contact with either wollastonite or calcite.   Clinopyroxene, quartz, and titanite are in contact with all the phases, and in Domain II, calcite is in contact with all the phases except scapolite.

(2)   Quartz in Domain I also forms minute grains and selvages between wollastonite and the garnet selvage surrounding wollastonite.

(3)   Some grains of scapolite surrounded by garnet in Domain II are partially replaced by a Pl-Cal-Kfs symplectite (Fig. 3c).

These textures suggest that the primary assemblages in Sample 2 were Wo-Pl-Qtz-Scp (Domain I) and Wo-Cal-Qtz-Scp (Domain II).   During a later event (or events), the primary assemblages were altered by the following reactions:

$$Wo + Pl \rightarrow Grt + Qtz, \qquad\qquad\qquad (1)$$
$$Wo + Scp + Cal \rightarrow Grt + CO_2, \qquad\qquad (2)$$
$$Scp \rightarrow Pl + Cal + Kfs. \qquad\qquad\qquad (3)$$

5.   Mineral Chemistry

The minerals were analyzed with a JEOL JCXA-733 electron microprobe at NIPR under conditions of a 15 kV accelarating voltage and a 0.012 μA specimen current.   The Bence-Albee correction method was used.   Two or more grains of each mineral per thin section were examined.   Representative analyses for Samples 1 and 2 are listed in Tables 2 and 3, respectively.   Analyses of Sample 1 are from three Domains A, B and C, which are selected in the direction across the gneissosity in the same thin section.   All three domains have the same mineral assemblage (Table 1).

5.1.   Garnet

Garnet compositions in both samples vary from grain to grain and from one analytical point to another within a given grain.   However, no systematic compositional zoning was found in the heterogeneous Sample 1 garnet.   Grossular ranges 80-91 mole % and is greatest in Domain A of Sample 1 (Fig. 4).   The remainder is mostly andradite (Fe_2O_3 ranges 3.8-7.3 wt%), whereas TiO_2, MnO and MgO are minor (<0.4, <0.8, <0.3 wt%, respectively) and Cr_2O_3 is negligible.

M. ASAMI, E.S. GREW and H. MAKIMOTO

Table 2. *Representative mineral analyses of a calc-silicate gneiss (Sample 1: MA88013009) from Austhamaren.*

Anal. No.	Domain A				Domain B				Domain C			
	Grt 9_3	Wo 5	Cpx 4	Cal 3	Grt 20	Wo 26	Cpx 22_2	Cal 24	Grt 28	Wo 31_2	Cpx 30	Ttn 35_2
SiO_2	38.67	50.99	51.46	0.00	38.49	50.03	50.90	0.00	38.02	50.97	49.84	29.92
TiO_2	0.08	0.04	0.00	0.02	0.21	0.00	0.00	0.00	0.25	0.04	0.00	32.72
Al_2O_3	21.16	0.00	0.41	0.00	20.83	0.03	0.56	0.01	20.14	0.00	0.42	3.73
Cr_2O_3	0.02	0.02	0.04	0.00	0.03	0.00	0.01	0.00	0.00	0.02	0.00	0.00
Fe_2O_3**	4.21				5.24				6.63			
FeO*		0.38	15.14	0.04		0.44	16.14	0.04		0.51	18.21	0.46
MnO	0.12	0.04	0.20	0.07	0.16	0.15	0.17	0.00	0.33	0.12	0.33	0.00
MgO	0.12	0.00	8.34	0.06	0.19	0.03	8.22	0.05	0.13	0.04	6.79	0.04
CaO	35.97	48.67	23.86	56.29	35.47	49.10	24.62	56.73	34.11	47.87	24.94	28.72
Na_2O	0.00	0.00	0.16	0.00	0.00	0.01	0.05	0.01	0.00	0.00	0.04	0.03
K_2O	0.01	0.00	0.02	0.00	0.03	0.00	0.00	0.03	0.01	0.00	0.00	0.01
Total	100.36	100.14	99.63	58.92	100.65	99.79	100.67	56.87	99.62	99.57	100.57	95.63
O	24	6	6	6	24	6	6	6	24	6	6	20
Si	5.876	1.979	1.996	0.000	5.853	1.958	1.969	0.000	5.870	1.987	1.957	4.073
Al	3.790	0.000	0.019	0.000	3.734	0.001	0.026	0.001	3.665	0.000	0.019	0.599
Ti	0.009	0.001	0.000	0.001	0.024	0.000	0.000	0.000	0.029	0.001	0.000	3.350
Cr	0.002	0.001	0.001	0.000	0.004	0.000	0.000	0.000	0.000	0.001	0.000	0.000
Fe^{3+}†	0.323				0.385				0.436			
Fe^{2+}	0.158	0.012	0.491	0.003	0.215	0.014	0.522	0.003	0.334	0.017	0.598	0.052
Mn	0.015	0.001	0.007	0.006	0.021	0.005	0.006	0.000	0.043	0.004	0.011	0.000
Mg	0.027	0.000	0.482	0.008	0.043	0.002	0.474	0.007	0.030	0.002	0.397	0.008
Ca	5.856	2.024	0.992	5.980	5.780	2.059	1.020	5.985	5.643	2.000	1.049	4.190
Na	0.000	0.000	0.012	0.000	0.000	0.001	0.004	0.002	0.000	0.000	0.003	0.008
K	0.002	0.000	0.001	0.000	0.006	0.000	0.000	0.004	0.002	0.000	0.000	0.002
	$Grs_{88.3}$	$Wo_{99.4}$	$Wo_{50.5}$		$Grs_{85.0}$	$Wo_{99.2}$	$Wo_{50.6}$		$Grs_{81.6}$	$Wo_{99.1}$	$Wo_{51.3}$	
	$Adr_{8.3}$	$En_{0.0}$	$En_{24.5}$		$Adr_{10.2}$	$En_{0.1}$	$En_{23.5}$		$Adr_{11.6}$	$En_{0.1}$	$En_{19.4}$	
	$Uvr_{0.1}$	$Fs_{0.6}$	$Fs_{25.0}$		$Uvr_{0.1}$	$Fs_{0.7}$	$Fs_{25.9}$		$Uvr_{0.0}$	$Fs_{0.8}$	$Fs_{29.2}$	
	$Alm_{2.6}$				$Alm_{3.6}$				$Alm_{5.6}$			
	$Prp_{0.5}$				$Prp_{0.7}$				$Prp_{0.5}$			
	$Sps_{0.3}$				$Sps_{0.3}$				$Sps_{0.7}$			

* Total iron as FeO. ** Total iron as Fe_2O_3. † Calculated for $Al^{vi}+Ti+Cr+Fe^{3+}=4$.

Table 3. Representative mineral analyses of a calc-silicate gneiss (Sample 2 : MA 88012206-2) from Eremitten.

Anal. No.	Domain I						Domian II						
	Pl 5	Scp 21	Wo 10	Cpx 7	Ttn 3	Grt 6	Scp 46	Wo 55	Cpx 51	Cal 60	Grt 45	Pl 49	Kfs 50
SiO_2	43.27	43.15	50.82	50.26	30.56	39.19	44.24	51.26	49.42	0.00	38.48	43.85	64.80
TiO_2	0.02	0.00	0.03	0.03	33.60	0.14	0.01	0.00	0.10	0.00	0.07	0.00	0.00
Al_2O_3	35.44	28.98	0.00	0.81	4.07	20.22	27.96	0.02	0.70	0.03	20.63	35.39	17.98
Cr_2O_3	0.00	0.00	0.00	0.00	0.06	0.00	0.00	0.02	0.02	0.04	0.01	0.00	0.00
Fe_2O_3**						6.17					5.72		
FeO*	0.08	0.12	0.28	16.85	0.41		0.01	0.20	19.00	0.02		0.00	0.00
MnO	0.04	0.00	0.20	0.44	0.00	0.56	0.00	0.12	0.82	0.03	0.68	0.03	0.00
MgO	0.00	0.01	0.01	7.29	0.01	0.11	0.00	0.03	5.36	0.02	0.12	0.00	0.00
CaO	19.18	20.48	48.85	23.59	28.41	34.52	19.78	48.99	23.81	54.73	34.73	19.23	0.05
Na_2O	0.89	2.29	0.00	0.25	0.00	0.00	2.86	0.00	0.06	0.06	0.05	0.66	0.47
K_2O	0.00	0.17	0.04	0.01	0.00	0.00	0.19	0.02	0.02	0.01	0.00	0.03	15.97
Total	98.92	95.20	100.23	99.53	97.12	100.91	95.05	100.66	99.31	54.94	100.49	99.19	99.27
O	32	Si+Al=12	6	6	10	24	Si+Al=12	6	6	6	24	32	32
Si	8.109	6.698	1.974	1.973	2.041	5.955	6.877	1.979	1.971	0.000	5.875	8.179	12.050
Al	7.829	5.302	0.000	0.037	0.320	3.621	5.123	0.001	0.033	0.004	3.713	7.781	3.941
Ti	0.003	0.000	0.001	0.001	1.688	0.016	0.001	0.000	0.003	0.000	0.008	0.000	0.000
Cr	0.000	0.000	0.000	0.000	0.003	0.000	0.000	0.001	0.001	0.003	0.001	0.000	0.000
Fe^{3+}†						0.408					0.403		
Fe^{2+}	0.013	0.015	0.009	0.553	0.023	0.297	0.001	0.006	0.634	0.002	0.254	0.000	0.000
Mn	0.006	0.000	0.007	0.015	0.000	0.072	0.000	0.004	0.028	0.003	0.088	0.005	0.000
Mg	0.000	0.002	0.001	0.426	0.001	0.025	0.000	0.002	0.319	0.003	0.027	0.000	0.000
Ca	3.852	3.406	2.033	0.992	2.033	5.620	3.294	2.027	1.018	5.976	5.682	3.843	0.010
Na	0.323	0.690	0.000	0.019	0.000	0.000	0.862	0.000	0.005	0.012	0.015	0.239	0.169
K	0.000	0.033	0.002	0.001	0.000	0.000	0.037	0.001	0.001	0.001	0.000	0.007	3.789
	$Or_{0.0}$ $Ab_{7.7}$ $An_{92.3}$	$Me_{83.2}$ $EqAn_{76.7}$	$Wo_{99.5}$ $En_{0.0}$ $Fs_{0.4}$	$Wo_{50.3}$ $En_{21.6}$ $Fs_{28.1}$		$Grs_{82.8}$ $Adr_{10.6}$ $Uvr_{0.0}$ $Alm_{5.0}$ $Prp_{0.4}$ $Sps_{1.2}$	$Me_{79.3}$ $EqAn_{70.8}$	$Wo_{99.6}$ $En_{0.1}$ $Fs_{0.3}$	$Wo_{51.7}$ $En_{16.2}$ $Fs_{32.2}$		$Grs_{83.5}$ $Adr_{10.3}$ $Uvr_{0.0}$ $Alm_{4.2}$ $Prp_{0.5}$ $Sps_{1.5}$	$Or_{0.2}$ $Ab_{5.8}$ $An_{94.0}$	$Or_{95.5}$ $Ab_{4.3}$ $An_{0.3}$

* Total iron as FeO.   ** Total iron as Fe_2O_3.   † Calculated for $Al^{VI}+Ti+Cr+Fe^{3+}=4$.

Grs

Grs

Sample 1:
MA88013009
Austhamaren

Sample 2:
MA88012206-2
Eremitten

o	Domain A
•	Domain B
△	Domain C

o	Domain I
•	Domain II

Adr

Alm+Prp+Sps

Alm+Prp+Sps

Fig. 4. Plots of garnet compositions on a Grs-Adr-(Alm + Prp + Sps) diagram.

Wo

Wo

Wollastonite

Sample 1:
MA88013009
Austhamaren

Sample 2:
MA88012206-2
Eremitten

Clinopyroxene

Clinopyroxene

o	Domain A
•	Domain B
△	Domain C

o	Domain I
•	Domain II

En

Fs

Fs
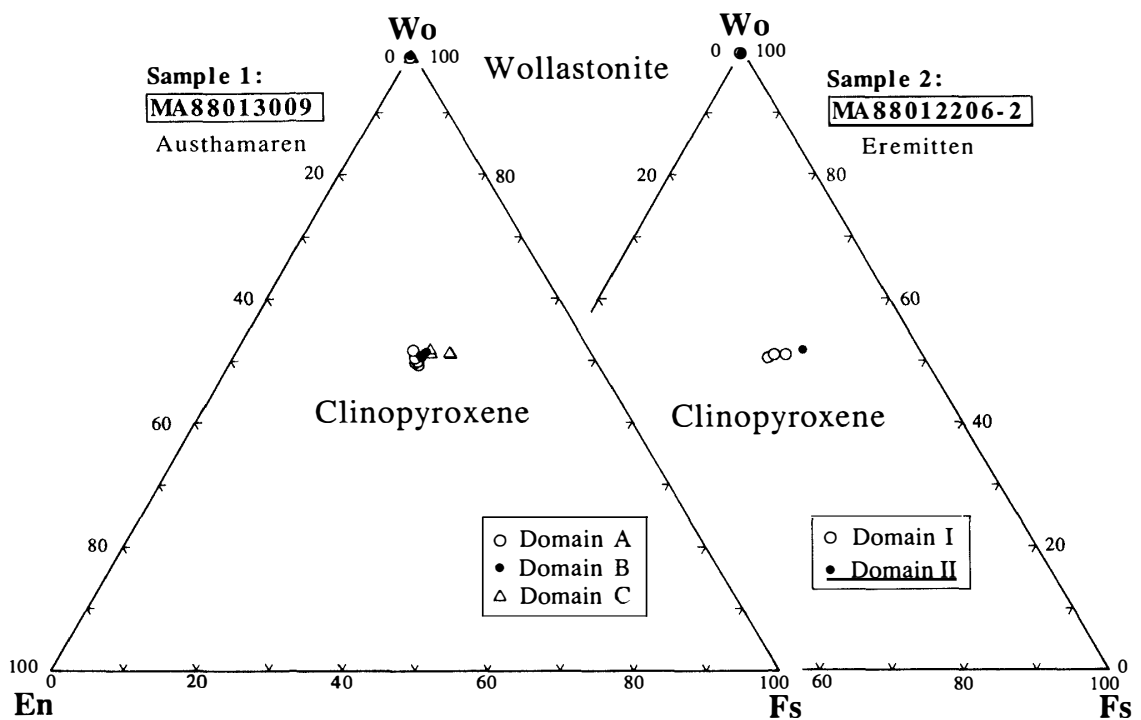
Fig. 5. Plots of wollastonite and clinopyroxene compositions on a Wo-En-Fs diagram.

Sample 2: MA88012206-2
Eremitten
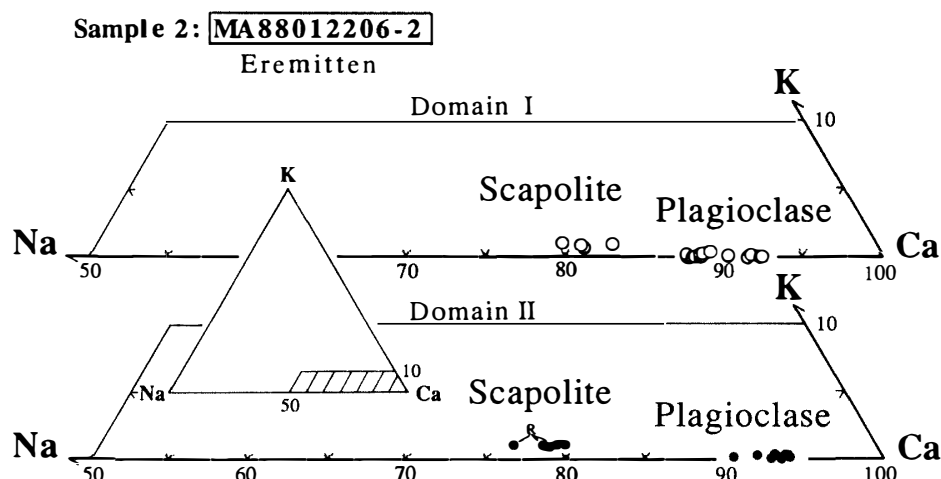
Fig. 6.   Plots of plagioclase and scapolite compositions on a K-Na-Ca diagram.
R : scapolite partially replaced by the Pl-Cal-Kfs symplectite.

5.2. Wollastonite

More than ten grains of wollastonite were analyzed in each sample.   In both samples, wollastonite compositions are very close to $CaSiO_3$ with minor FeO (<0.6 wt%) and MnO (<0.3 wt%) (Fig. 5).

5.3. Clinopyroxene

Clinopyroxene in both samples is hedenbergite ($X_{Fe} = Fe/(Fe+Mg) = 0.50$–0.61 in Sample 1 ; 0.57–0.67 in Sample 2) (Fig. 5), with low contents of TiO_2 (<0.1. wt%), Al_2O_3 (<1.0 wt%), Cr_2O_3 (<0.1 wt%), MnO (<0.8 wt%) and Na_2O (<0.3 wt%).

5.4. Plagioclase and K-feldspar

Primary plagioclase in Domain I of Sample 2 is An_{88-92}, less calcic than secondary plagioclase (An_{90-94}) in the symplectites replacing scapolite in Domain II (Fig. 6).   The primary plagioclase is compositionally heterogeneous, but no systematic zoning was found.

K-feldspar in the Pl-Cal-Kfs symplectite from Sample 2 is Or_{95-96}.

5.5. Scapolite

Domain II scapolite (Me_{77-80}, $EqAn*_{71-75}$) is more sodic than Domain I scapolite (Me_{80-83}, $EqAn_{72-77}$) (Fig. 6).   In Domain II, the scapolites which are partially replaced by symplectite are more sodic (Me_{77-79}) than scapolite (Me_{80}) grains that have not been replaced by symplectite.

Scapolite contains minor K_2O (Table 2 and Fig. 6), which would explain the appearance of K-feldspar in the symplectite.   SCHENK (1984) and MOTOYOSHI et al. (1991) reported similar symplectites except that quartz was present instead of K-feldspar.

The Pl-Cal-Kfs symplectite + Na-richer scapolite association, which is enclosed

---

* Equivalent anorthite content :   100 (Al-3)/3 (ELLIS, 1978).

in garnet selvages, is estimated (using the data of Oterdoom and Gunter, 1983) to have formed from Ca-richer scapolite by the continuous reaction (3) at $\leq 600°C$.

5.6. Calcite and titanite

Calcite is near end-member $CaCO_3$. Titanite contains substantial Al_2O_3.

6. Petrogenetic Significance

6.1. Granulite-facies metamorphism

The most important difference between the assemblages in Samples 1 and 2 is the presence of Grt-Qtz-Cal in the former and Wo-Pl-Scp and Wo-Cal-Scp in the latter. In both cases, the minerals approach end-member compositions, that is, Grs and An contents reach 90% in garnet and plagioclase, respectively. Reactions (1) and (2) relate the assemblages in these two samples.

Reaction (1) has been widely applied to estimate P-T conditions of granulite-facies metamorphism, including Antarctica (Asami and Shiraishi, 1985; Hiroi et al., 1987; Motoyoshi et al., 1991). The end-member reaction Grs+Qtz=Wo+An, together with the effects of andradite=grossular and Ab=An substitutions, have been experimentally investigated (Windom and Boettcher, 1976; Huckenholz et al., 1981). The experimental data indicate that 10% albite shifts the reaction curve to lower temperatures by about 10°C, whereas 10% andradite shifts it to higher temperatures by about 5°C, that is, the effects roughly cancel each other, and the end-member reaction is applicable as a first approximation (Fig. 7).

Temperatures and pressures estimated for granulite-facies in the eastern Sør Rondane Mountains are 760-800°C and 7-8 kbar (Grew et al., 1989a; Makimoto et al., 1990; Asami and Makimoto, 1991; Makimoto and Asami, 1991; Asami et al., 1992), and the P-T range is depicted in Fig. 7 together with the P-T-t path of metamorphism in the Sør Rondane Mountains. At these temperatures, Grt-Qtz would be stable at 7-8 kbar, whereas Wo+An would only be stable at less than 7 kbar. A regional decrease in pressure southward from Austhamaren to Eremitten is suggested by the distribution of Grt-Cpx assemblages in mafic rocks (Fig. 1). However, appearance of the Grt-Cpx assemblage is very sensitive to bulk composition, and the garnet-bearing mafic rocks in the eastern Sør Rondane Mountains are highly variable in composition. For example, Fe-rich varieties are found at Austhamaren, Mg-rich varieties in central Balchenfjella (Grew et al., 1989a). Thus, there is little evidence for P gradients in the eastern Sør Rondane.

Alternatively, the combination of a difference in CO_2 activity and subtle differences (e.g., Fe/Al or Na/Ca ratio) in bulk composition between the two rocks could account for the different assemblages. For example, at constant P and T, assemblages with Wo+Scp form at higher CO_2 activities than Grs+Qtz (reaction (2)). If Harley and Buick's (1992, Fig. 11a) P-a_{CO_2} plot for $T = 850°C$ can be applied to the Sør Rondane, it can be shown that Wo-An-Scp (in a somewhat more sodic bulk composition), Wo-Cal-Scp, and Grt-Qtz-Cal could be stable at roughly the same pressure, with the last assemblage at lower a_{CO_2} than the other two assemblages. The lower a_{CO_2} could have resulted from the contact effect of the ortho-
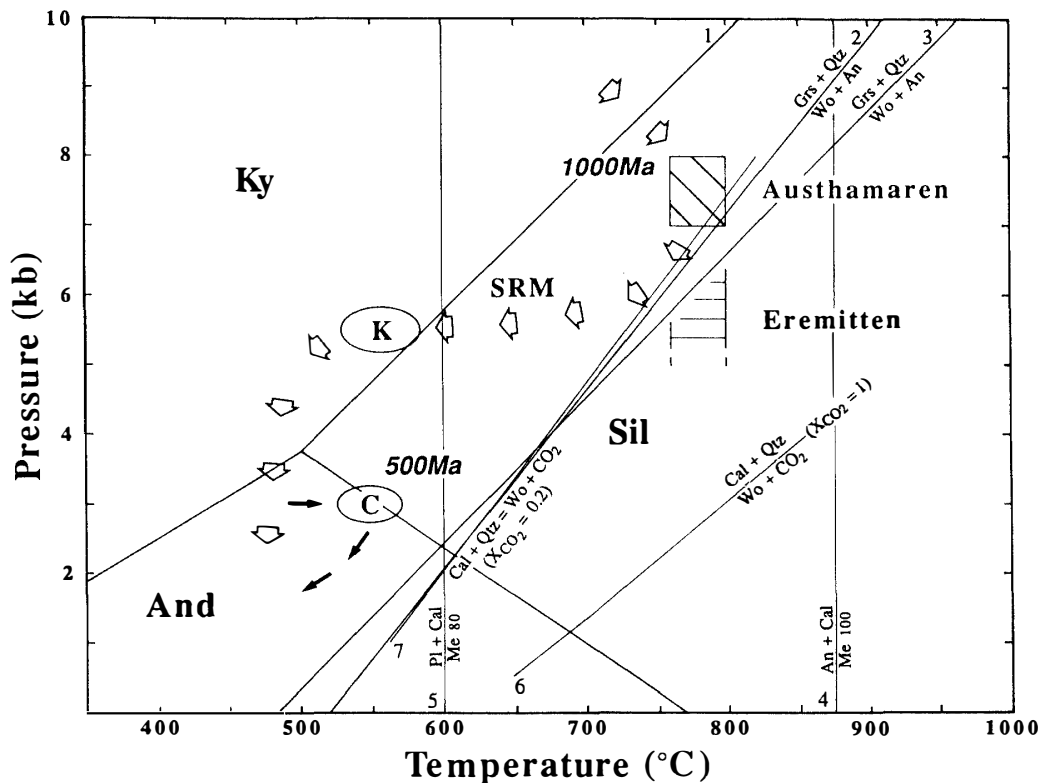
Fig. 7. P-T diagram showing the positions of the Austhamaren Grt-Qtz assemblage and Eremitten Wo-An assemblage relative to the end-member reaction $Grt + Qtz = An + Wo$. A P-T-t path for the Sør Rondane metamorphism (SRM)) (ASAMI et al., 1992) is also shown ; K : P-T conditions of the kyanite-forming retrograde episode ; C : P-T conditions of the contact metamorphism and migmatization. Reaction curves : 1-HOLDAWAY (1971) ; 2-WINDOM and BOETTCHER (1976) ; 3-HUCKENHOLZ et al., (1981) ; 4-GOLDSMITH and NEWTON (1977) ; 5-OTERDOOM and GUNTER (1983) ; 6-HARKER and TUTTLE (1956) ; 7-GREENWOOD (1967).

gneiss, which during intrusion would have driven off some CO_2 from the calc-silicate rock prior to the regional granulite-facies metamorphism.

Both samples 1 and 2 (Domain II) contain the CO_2-buffering assemblage, Wo-Cal-Qtz. According to the T-X_{CO_2} phase relations in the CaO-Al_2O_3-SiO_2-H_2O-CO_2 system at $P = 7$ kbar compiled by HIROI et al. (1987, Fig. 9b), X_{CO_2} would have been buffered at < 0.3 in the assemblage with scapolite and at 0.1-0.2 in the assemblage with grossular for $T = 760$-$800°C$ (Fig. 7). Such low X_{CO_2} values and preservation of CO_2-buffering assemblages, together with variations in X_{CO_2} from layer to layer and within a layer (e.g., the 0.5 m thick marble at Austhamaren contains Cal-Qtz with no Wo), argue strongly against CO_2 infiltration as a mechanism in granulite-facies metamorphism (HARLEY and BUICK, 1992) in the eastern Sør Rondane Mountains.

6.2. Retrograde metamorphism

Garnet selvages and Pl-Cal-Kfs symplectites in the Eremitten calc-silicate gneiss indicate recrystallization after peak metamorphic conditons, possibly in two stages.

Formation of garnet rims between scapolite and wollastonite could have resulted from a near-isobaric decrease of temperature at relatively low X_{CO_2} (Harley and Buick, 1992). Further decrease in temperature (to $< 600°C$, see above) resulted in scapolite (Me_{80}) breakdown to $Pl + Cal$ ($+ Kfs$), a CO_2-conservative reaction (Fig. 7). There is little evidence in the Eremitten calc-silicate gneiss for the hydration that resulted in partial replacement of clinopyroxene by hornblende and of orthopyroxene by cummingtonite in some associated mafic rocks.

Acknowledgments

References

Asami, M. and Shiraishi, K. (1985): Retrograde metamorphism in the Yamato Mountains, East Antarctica. Mem. Natl Inst. Polar Res., Spec. Issue, **37**, 147–163.

Asami, M. and Makimoto, H. (1991): Granulite-facies metamorphic conditions in the eastern Sør Rondane Mountains, East Antarctica (abstract). Proc. NIPR Symp. Antarct. Geosci., **5**, 166.

Asami, M., Makimoto, H. and Grew, E.S. (1989): Geology of the eastern Sør Rondane Mountains, East Antarctica. Proc. NIPR Symp. Antarct. Geosci., **3**, 81–99.

Asami, M., Grew, E.S. and Makimoto, H. (1990): A staurolite-bearing corundum-garnet gneiss from the eastern Sør Rondane Mountains, Antarctica. Proc. NIPR Symp. Antarct. Geosci., **4**, 22–40.

Asami, M., Makimoto, H., Grew, E.S., Osanai, Y., Takahashi, Y., Tsuchiya, N., Tainosho, Y. and Shiraishi, K. (1991): Geological map of Balchenfjella, Sør Rondane Mountains, Antarctica. Antarctic Geological Map Series, Sheet 31 (with explanatory text 11 p., 8 pl.). Tokyo, Natl Inst. Polar Res.

Asami, M., Osanai, Y., Shiraishi, K. and Makimoto, H. (1992): Metamorphic evolution of the Sør Rondane Mountains, East Antarctica. Recent Progress in Antarctic Earth Science, ed. by Y. Yoshida et al. Tokyo, Terra Sci. Publ., 7–15.

Ellis, D.E. (1978): Stability and phase equilibria of chloride and carbonate bearing scapolite at 750°C and 4000 bar. Geochim. Cosmochim. Acta, **42**, 1271–1281.

Goldsmith, J.R. and Newton, R.C. (1977): Scapolite-plagioclase stability relations at high pressures and temperatures in the system $NaAlSi_3O_8$-$CaAl_2Si_2O_8$-$CaCO_3$-$CaSO_4$. Am. Mineral., **62**, 1063–1081.

Greenwood, H.J. (1967): Wollastonite: stability in H_2O-CO_2 mixtures and occurrences in a contact-metamorphic aureole near Salmo, British Columbia. Am. Mineral., **52**, 1669–1680.

Grew, E.S., Asami, M. and Makimoto, H. (1988): Field studies in the eastern Sør Rondane Mountains, East Antarctica, with the 29th Japanese Antarctic Research Expedition (JARE). Antarct. J. U. S., **23**(5), 44–46.

Grew, E.S., Asami, M. and Makimoto, H. (1989a): Preliminary petrological studies of the metamorphic rocks of the eastern Sør Rondane Mountains. Proc. NIPR Symp. Antarct. Geosci., **3**, 100–127.

GREW, E.S., ASAMI, M. and MAKIMOTO, H. (1989b) : A luminous and manganoan titanite from the Sør Rondane Mountains, East Antarctica. Antarct. J.U.S., **24**(5), 42-43.

GREW, E.S., ESSENE, E.J., PEACOR, D.R., SU, S. and ASAMI, M. (1991) : Dissakisite-(Ce), a new member of the epidote group and the Mg analogue of allanite-(Ce), from Antarctica. Am. Mineral., **76**, 1990-1997.

GREW, E.S., MANTON, W.I., ASAMI, M. and MAKIMOTO, H. (1992) : Reconnaissance geochronologic data on Proterozoic polymetamorphic rocks of the eastern Sør Rondane Mountains, East Antarctica. Recent Progress in Antarctic Earth Science, ed. by Y. YOSHIDA *et al.* Tokyo, Terra Sci. Publ., 37-44.

HARKER, R.I. and TUTTLE, O.F. (1956) : Experimental data on the P_{CO_2}-T curve for the reaction : calcite + quartz = wollastonite + CO_2. Am. J. Sci., **254**, 239-256.

HARLEY, S.L. and BUICK, I.S. (1992) : Wollastonite-scapolite assemblages as indicators of granulite pressure-temperature-fluid histories : The Rauer Group, East Antarctica. J. Petrol., **33**, 693-728.

HIROI, Y., SHIRAISHI, K., MOTOYOSHI, Y. and KATSUSHIMA, T. (1987) : Progressive metamorphism of calc-silicate rocks from the Prince Olav and Sôya Coasts, East Antarctica. Proc. NIPR Symp. Antarct. Geosci., **1**, 73-97.

HOLDAWAY, M.J. (1971) : Stability of andalusite and the aluminium silicate phase diagram. Am. J. Sci., **271**, 97-131.

HUCKENHOLZ, H.G., LINDHUBER, W. and FEHR, K.T. (1981) : Stability relationships of grossular + quartz + wollastonite + anorthite. I. The effect of andradite and albite. Neues Jahrb. Mineral. Abh., **142**, 223-247.

MAKIMOTO, H. and ASAMI, M. (1991) : Metadikes in the eastern Sør Rondane Mountains, East Antarctica (abstract). Proc. NIPR Symp. Antarct. Geosci., **5**, 167.

MAKIMOTO, H., ASAMI, M. and GREW, E.S. (1990) : Metamorphic conditions of ultramafic lenses from the eastern Sør Rondane Mountains, East Antarctica. Proc. NIPR Symp. Antarct. Geosci., **4**, 9-21.

MOTOYOSHI, Y., THOST, D.E. and HENSEN, B.J. (1991) : Reaction textures in calc-silicate granulites from the Bolingen Islands, Prydz Bay, East Antarctica : Implications for the retrograde *P-T* path. J. Metamorphic Geol., **9**, 293-300.

KRETZ, R. (1983) : Symbols for rocks-forming minerals. Am. Mineral., **68**, 277-279.

OTERDOOM, W.H. and GUNTER, W.D. (1983) : Activity models for plagioclase and CO_2-scapolite —An analysis of field and laboratory data. Am. J. Sci., **283-A**, 255-282.

SCHENK, V. (1984) : Petrology of felsic granulites, metapelites, metabasics, ultramafics, and metacarbonates from southern Calabria (Italy) : Prograde metamorphism, uplift and cooling of a former lower crust. J. Petrol., **25**, 255-298.

SHIRAISHI, K. and KAGAMI, H. (1992) : Sm-Nd and Rb-Sr ages of metamorphic rocks from the Sør Rondane Mountains, East Antarctica. Recent Progress in Antarctic Earth Science, ed. by Y. YOSHIDA *et al.* Tokyo, Terra Sci. Publ., 29-35.

WINDOM, K.E. and BOETTCHER, A.L. (1976) : The effect of reduced activity of anorthite on the reaction grossular + quartz = anorthite + wollastonite : A model for plagioclase in the earth's lower crust and upper mantle. Am. Mineral., **61**, 889-896.